High-speed camera visualizations of flame acceleration in a square channel with obstacles: the case of binary fuels H_2/C_3H_8-Air mixture

Guanbing CHENG, Ratiba ZITOUN, Yves SARRAZIN, Alain CLAVERIE, Pierre VIDAL, Bernard VEYSSIERE, Pascal BAUER

Institut P' UPR 3346, Département Fluides, Thermique, Combustion, CNRS
1 Av. Clément Ader, BP 40109, 86961 Futuroscope, FRANCE

1 Introduction

Because of the increasing consumption of fossil fuels and associated environmental concerns, more attention has been paid on hydrogen utilization since its combustion products do not contain hydrocarbons and carbon dioxide. However, its greater flammability and propensity to leak, and its low ignition energy make the practical use of hydrogen in industrial production, storage and distribution, an important safety issue. Explosion hazards in the hydrogen industry are often considered to be associated with the onset of detonation or **Deflagration-to-Detonation Transition** (***DDT***) following flame acceleration. The flame acceleration depends not only on the reactivity of the mixtures, but also on the dimensions of the experimental set-up, the obstacles and the magnitude of ignition energy [1]. Adding an inhibitor (e.g. methane or propane) is considered as a solution for handling safety issues in industrial applications of H_2/Air mixtures. It is thus of important interest to identify the mechanism of flame acceleration in such binary fuels mixtures.

Ciccarelli et al.[2] carried out an experimental study about the effects of different blockage ratios B.R, obstacle spacing and mixture equivalence ratio Φ on the initial stage of the stoichiometric propane-air flame acceleration. They considered obstacles made up of orifice plates distributed along the tube. They found that flame acceleration in the tube with the higher B.R obstacles is greater when the obstacle spacing corresponds to the tube diameter. However, for lower B.R obstacles, they found no significant effect of spacing on this accelerating period. They obtained an optimum flame acceleration condition when the length of recirculation zone between the adjacent obstacles in the unburned gas is comparable with the obstacle spacing. With a novel Schlieren method, Johansen et al.[3] and Cicarrelli et al.[4] performed visualizations of flame acceleration in stoichiometric methane-air mixtures in an obstructed square channel. They observed that the first acceleration stage is due to flame area enhancement resulting from large-scale flame distortion and small-scale turbulence wrinkling downstream of obstacles. The later stages are mainly governed by the interaction of flame-shock interactions and flow contraction through the obstacle pairs.

To our knowledge, only few works address flame acceleration in such binary fuels H_2/C_3H_8-Air mixtures. Law et al.[5] studied hydrocarbon addition to inhibit explosion hazards and found that small or moderate addition of propane effectively reduced laminar burning velocities and restrained the possibility of diffusional, thermal and hydrodynamic cellular instabilities in H_2/air flames. More recently, Sorin et al.[6], Bozier et al.[7] and Cheng et al.[8-9] have determined detonation characteristics of binary fuels H_2/CH_4-Air and H_2/C_3H_8-Air mixtures and the ***DDT*** run-up distances from pressure signals without visualization.

The present paper is a further work of our previous studies [8-9]. It focuses on the visualization by a shadow method of the initial stage of the flame acceleration in the H_2/C_3H_8-Air mixtures in a square channel laden with obstacles. The mixture composition and the molar fraction *x* are given by: Φ [x H_2+ (1-x) C_3H_8] + (5–4.5x) (O_2 + 3.76 N_2), $x = H_2/(H_2 + C_3H_8)$.This paper reports on the first results, which are relative to an equivalence ratio Φ=1.1, molar fraction of hydrogen x=0.9 and 0.95, initial temperature 293 K, and initial pressures Pi=0.5 bar and 1 bar.

2 Experimental set-up

Experiments are performed in a stainless-steel channel with 40-mm×40-mm square cross-section and 4-m length. The channel is made up of 8 sections about 50-cm length. Two sections located at the beginning of the tube are equipped with glass windows for visualization. Nine piezoelectric pressure transducers (KISTLER 603B, 1 μs rise time) are distributed along the channel. One is located on the first optical section, at 35 cm from the ignition point, two on the second optical section, 25-cm apart, the first at 12.5 cm from the end of the first optical section. The flame is accelerated by an array of periodical obstacles with B.R=0.5 located along the first half of the channel. The obstacles are the square plates with a 31-mm diameter orifice; their spacing is equal to the tube inner diameter and the thickness is 8 mm. The mixtures are ignited by an automotive spark plug with about 15-mJ discharge energy.

A typical Z-shadow system is used for visualization. The optical set-up is made up of a 500-Watt mercury vapor arc lamp (HC500W2O), two 45-cm diameter parabolic mirrors with 4-m focal length, and a high-speed digital camera Photron APX RS3000. The camera was operated with a 1-μs shutter time, 17500 frames per second, and a spatial pixel resolution of 1028×176. The visualization domain extends over about six obstacles from the ignition point.

3 Results and discussion

The high-speed shadow images of the flame acceleration given in Fig.1 show the flame acceleration for two different initial pressures. After ignition, the flame has hemispherical shape, convex to the fresh unburned mixtures. Its radius increases until its arrival on the channel inner surface. At t=1.486 ms, the flame is at mid-span of spacing between the ignition point and the 1st obstacle. Due to confinements of channel wall, the flame begins to contract and seems to develop to the so-called "tulip flame". The flame center line-velocity increases as the fresh gas flow contracts to the obstacle orifice. Once the flame-tip passes through the first obstacle, a turbulent combustion appear downstream the obstacle. It corresponds to "the flame rolls up in vortices" observed by Johansen et al.[3] and Ciccarelli et al.[4]. However, the core flame tip remains laminar. The flame area is greatly increased and accordingly increases the volumetric burning rates which in turn increase the flame velocity. This feedback mechanism is observed at the next obstacles. It results in high acceleration of the flame tip. The velocity reached is 600 m/s at 1bar and 450 m/s at 0.5bar. However, for 1 bar, at t=3.086 ms, the flame presents multi-structure outline at the exit of the second obstacle and compression waves seem to occur downstream of 4th obstacle at t=3.371 ms.

Fig.2 shows the visualization obtained for x=0.9 at Pi=1bar. We can observe that the propane addition significantly reduces the flame velocity. At t=3.543 ms, for instance, the flame passes through the 5th obstacle for x=0.95, however it just exits the 1st obstacle for x=0.9. The flame acceleration mechanisms are nearly the same as those observed in Fig.1. The flame acceleration results from the growth of the flame surface due to the flow contraction at the obstacle orifice and to the turbulent combustion in the recirculation zone behind the flame front. Compression waves in the unburned gas are also observed at the exit of the 4th obstacle.

To better analyze the variations of the initial period of flame propagation, the average flame tip velocities as a function of distance from the ignition point are plotted in Fig.3 at Pi=1.0 bar (red square points) and Pi=0.5 bar (pink points). The square points in the horizontal coordinate represent different positions of obstacles along the channel. From the Fig.3, we can observe that the flame tip velocity increases just before it passes through the obstacles and decreases during the first mid-span obstacles spacing. In the distance from the ignition point to the 4th obstacle, there is no significant influence of initial pressure on the flame acceleration and it seems to be independent of initial pressure. After the 4th obstacle, the flame tip velocities in the two cases increase monotonically probably due to the effect of compression wave in the unburned gas.

Fig.4 represents the variation of the flame tip velocity as a function of distance X from ignition point along the length of the channel. The results show that the addition of propane reduces the flame velocities. The flame velocity increases similarly just before the flame passes through the obstacles and decreases in the first mid-span obstacle spacing.

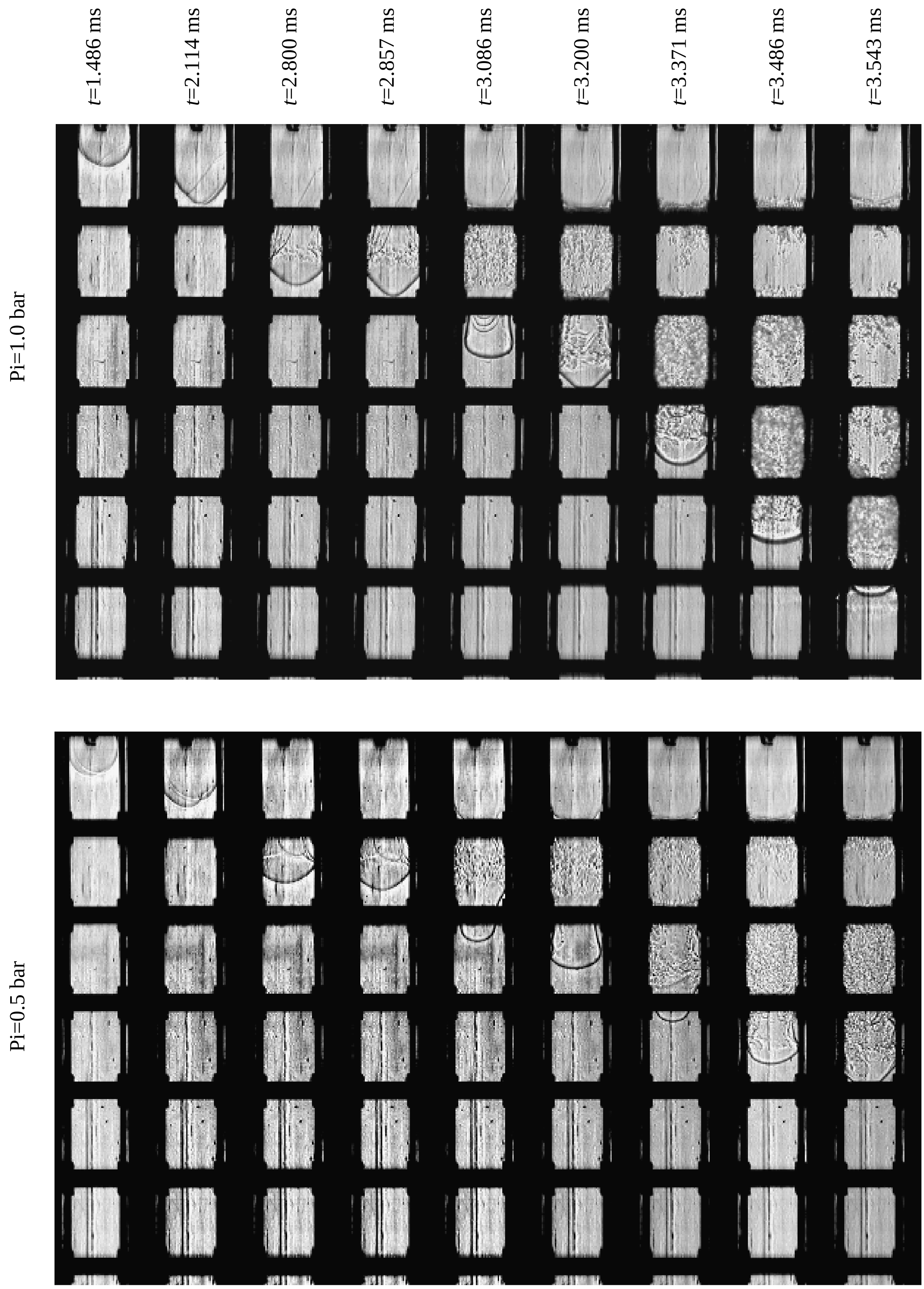

Figure 1. High speed shadow photography images of flame acceleration of H_2/C_3H_8-Air mixtures (Φ=1.1 and x=0.95) at different initial pressures (0.5 bar and 1.0 bar for Φ=1.1)

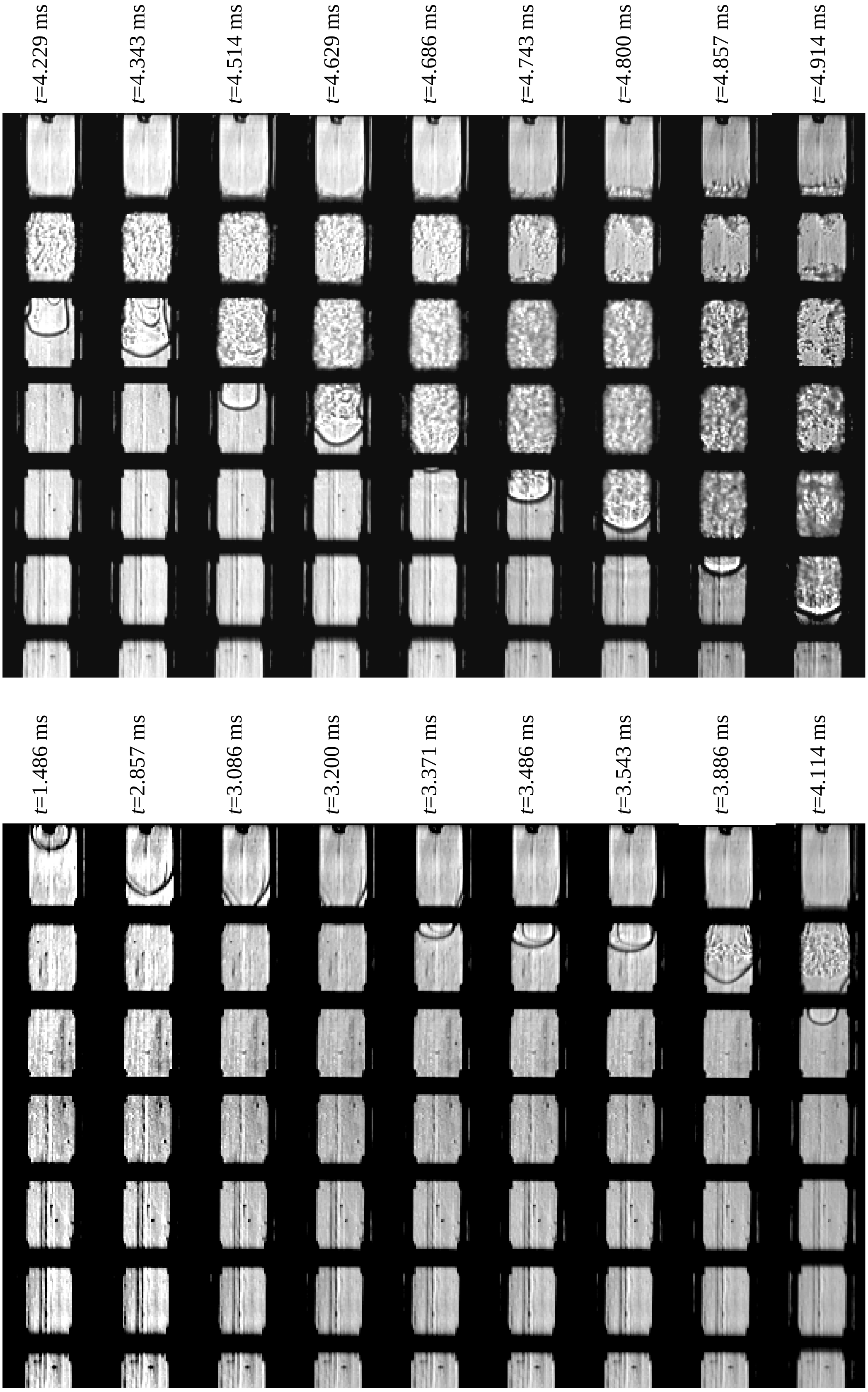

Figure 2. High speed shadow photography images of flame acceleration of H_2/C_3H_8-Air mixtures (x=0.9 and 0.95 for Φ=1.1)

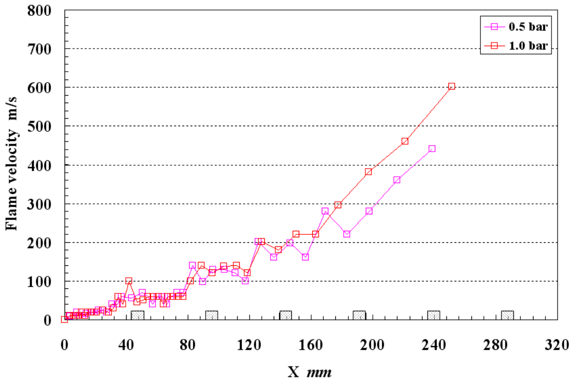

Figure 3. Flame velocity as a function of distance X for different initial pressure Pi

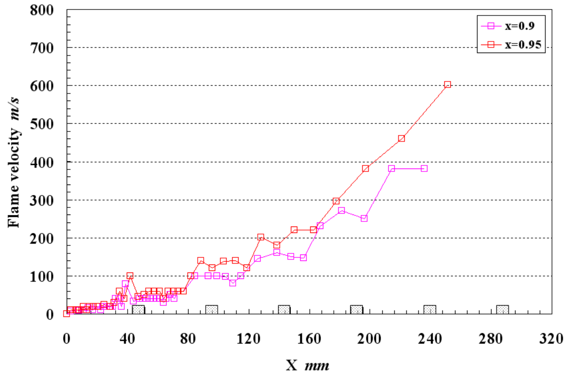

Figure 4. Flame velocity as a function of distance X for different hydrogen molar fraction *x*

Conclusions

In this paper, we have performed visualization of initial stage of flame acceleration in H_2/C_3H_8-Air mixtures using shadow technique with high speed camera. The experiments are carried out in an obstacle-filled stainless steel channel with 40 mm×40 mm square cross-section and 4-m length at the room temperature with two initial pressures (Pi=0.5 bar and 1 bar) and H_2 molar fractions x (Φ=1.1; x=0.9 and 0.95). The results show that the acceleration flame results from the contraction of unburned flow near obstacle and from delayed turbulent combustion in recirculation zone behind the flame front. The evolutions of measured flame velocities are due to the acceleration or deceleration of the unburned gas which passes through the obstacles. For different x, we obtain the nearly same variation of flame velocity (x=0.9 at Pi=1bar) as those in mixtures (x=0.95 at Pi=1bar). It should be noted that the addition of propane in such binary fuels mixtures significantly reduces the flame velocity.

References

[1] S.Kerampran (2000). Etude des mécanismes d'accélération des flammes se propageant depuis l'extrémité fermée vers l'extrémité ouverte de tubes horizontaux de longueur variable. PhD thesis, University of Poitiers, Poitiers,France.

[2] G.Ciccarelli, C.Fowler, M.Bardon (2005). Effect of obstacle size and spacing on the initial stage of flame acceleration in a rough tube. Shock Wave 14(2):161-166.

[3] C.T.Johansen, G.Ciccarelli (2008). Visualization of the unburned gas flow field ahead of an accelerating flame in an obstructed square channel. Combustion and flame 156:405-416.

[4] G.Ciccarelli,C.T.Johansen,M.Parravani (2010). The role of shock-flame interactions on flame acceleration in an obstacle laden channel. Combustion and flame 157(11): 2125-2136.

[5] C.K.Law, O.C.Kwon (2004). Effects of hydrocarbon substitution on atmospheric hydrogen-air flame propagation. Inter. Journal of hydrogen and energy 29:867-879.

[6] R.Sorin, O.Bozier, R.Zitoun, D.Desbordes. (2009). Deflagration to detonation transition in binary fuels H_2/CH_4 with air mixtures. Proc.22nd ICDERS, paper 186.

[7] O.Bozier, R.Sorin, R.Zitoun, D.Desbordes. (2009). Detonation characteristics of H_2-natural gas-air mixtures. Proc. European Combustion Meeting, Vienna, Australia. Paper 167.

[8] G.CHENG, R.ZITOUN. (2010). Detonation characteristics of the binary mixtures H_2/C_3H_8-air. WIP abstract of 33rd Inter. Symp. on Combustion: W4P114.

[9] G.CHENG, R.ZITOUN. (2011). Deflagration-detonation transition in tube filled with binary mixtures H_2/C_3H_8-Air. Proc. European Combustion Meeting, Cardiff, UK.